IEEE Access
Multidisciplinary | Rapid Review | Open Access Journal

Received 28 September 2022, accepted 9 October 2022, date of publication 14 October 2022, date of current version 26 October 2022.

Digital Object Identifier 10.1109/ACCESS.2022.3214831

APPLIED RESEARCH

Fin-Rudder Joint Control Based on Improved Linear-Quadratic-Regulator Algorithm

YUHAN ZHAO, ZHANSHUO ZHANG, JIAWEI WANG, AND HONGBO WANG
State Key Laboratory on Integrated Optoelectronics, College of Electronic Science and Engineering, Jilin University, Changchun 130012, China
Corresponding author: Hongbo Wang (wang_hongbo@jlu.edu.cn)

This work was supported in part by the National Natural Science Foundation of China (NSFC) under Grant u1964202.

ABSTRACT Navigation accidents and disasters frequently occur when ships sail at sea owing to extreme weather, wind, and wave conditions. The disturbance of wind and waves affects the stability of the ship's course and makes the ship roll violently. Ships are usually equipped with an autopilot to control the course and a fin stabilizer to reduce rolling during navigation and improve stability and safety. Fin-rudder joint control system considers the coupling effect of the ship's horizontal plane motion, thereby improving the performance of the rudder and the fin stabilizer. This paper presents an improved linear-quadratic-regulator control algorithm. A rate control law with no static error is proposed based on the traditional linear-quadratic-regulator to eliminate the static error of the state vector and achieve a better control effect. Additionally, a closed-loop state observer is used to estimate the system's state vector, and a dynamic corrector is designed to reduce rolling and heading angle deviation caused by sea wave interference. The simulation results show that the designed fin-rudder joint controller with the improved linear-quadratic-regulator algorithm can achieve more than 80% roll reduction effect at level 3 and 5 sea states, and has better course keeping ability compared with the rudder control.

INDEX TERMS Fin-rudder joint control, linear-quadratic-regulator (LQR), roll reduction, rate control law with no static error, dynamic corrector.

I. INTRODUCTION

The rapid development of the shipping industry has contributed to the frequent marine accidents worldwide. The requirements for ship sailing control are also rising to reduce marine accidents [1]. When a ship is sailing at sea, the rolling movement caused by wind, waves, and other environmental disturbances reduces the ship's stability and compromises navigational safety [2]. Similarly, under the interference of sea waves, a ship produces a sway of heading, causing ship deviation the heading and possibly collision accidents [3]. Therefore, controlling a ship's heading and reducing its rolling motion is of great significance to ensure the stability of the ship's navigation and reduce maritime accidents [4].

Over the years, the researchers from various countries have designed various anti-rolling devices such as fin stabilizers, antirocking tank and bilge keels to ensure the stability and safety of ships [5]. The fin stabilizer is the most used anti-rolling device with good effect. By controlling the movement of the fin, an anti-rolling moment is generated to offset the rolling moment of the wave acting on the ship [6], [7]. The anti-rolling moment generated by the fin is proportional to the square of the speed of the ship. Therefore, the anti-rolling effect of the fin stabilizer is constrained by the speed of the ship. The performance of the fin stabilizer is greatly reduced when the rate is very low [8], [9]. In 1970, Taggart [10] showed that the autopilot controls the heading motion via steering and causes the roll angle to change. Taggart believed that manipulating the autopilot could reduce the rolling motion caused by the disturbance of the waves. This method is called rudder roll reduction (RRS). Rudder antiroll is economically advantageous because it only requires adding an antiroll control link to the steering gear; however, its disadvantage is that it quickens the wear of the steering gear [11]. Carley and Duberley [12] first proposed the joint fin-rudder control in 1972 to address the limitations

The associate editor coordinating the review of this manuscript and approving it for publication was Okyay Kaynak.

of autopilot and stabilizer fin. The joint fin-rudder control takes advantage of the fact that steering can simultaneously produce roll and heading motion. The autopilot and fin stabilizers are combined to conduct comprehensive control of ship motion, with the fin stabilizer playing the main role in roll reduction and the autopilot playing an auxiliary role while maintaining the course by considering the coupling between heading and rolling [13]. Hongzhang [14] established a mathematical model of the fin-rudder joint control system with integral signals. They further designed an optimal controller with an integrator using the linear-quadratic-gaussian (LQG) control theory, which achieved a better control effect. Liang et al. [15] designed a fin-rudder joint roll reduction system with H_∞ robust control method and proportional-integral-derivative (PID) autopilot in heading control. Their simulation results showed that the independent heading control and roll reduction achieved good results. Li et al. [16] designed a sliding mode controller based on input and output feedback linearization and simulated rolling and heading joint control under different sea conditions. Their simulation results showed the controller's robustness and better roll stability while maintaining heading control accuracy. Liang et al. [17] designed a distributed model predictive controller for fins and rudder joint control. Their simulation results show that the constrained control ensures the control performance of ships in harsh sea conditions and improves roll stability on the premise of maintaining heading stability. The commonly used controllers highlighted above have some advantages and disadvantages:

- H_∞ robust controller: nonlinear controller with strong robustness in which the system generally works in a nonoptimal state, so the steady-state accuracy of the system is low.
- Sliding model controller: nonlinear controller with strong robustness and insensitivity to disturbance and model error in which a "chattering" phenomenon occurs when the system reaches equilibrium.
- PID controller: the most widely used in the engineering field at present. It does not need to know the model of the system, and only adjusts according to the deviation between the expectation and the status quo, so that it can reach the desired linear controller. Compared with PID, LQR can take into account multiple performance indicators.
- MPC controller: it is good at dealing with MIMO systems and prediction and rolling optimization characteristics but requires heavy calculations and sacrifices certain optimality compared with the linear-quadratic-regulator (LQR). Compared with MPC, LQR has faster response and higher tracking efficiency when the system is not disturbed [18].

Among these common control algorithms, LQR has been selected as the most effective, simple application and popular controller. It is a well-known systematic design technique for optimal control of linear systems that can minimize a quadratic cost function establishing a reasonable balance between the reduction of responses and required control forces [19], [20], [21].

This study designs a rate control law with no static error based on the optimal control solution obtained from traditional LQR. The design of the rate control law with no static error ensures the basic law of optimality and realizes the system state vector of no static error. A dynamic corrector is designed to reduce the influence of wave disturbance on heading angle and roll angle.

The rest of this paper is organized as follows: The building of the ship and actuator model is described in section II. The control method and controller design are introduced in section III. Section IV shows the simulation results and data to validate the performance of the improved control algorithm. Finally, the conclusion is presented in section V.

II. MATHEMATICAL MODEL

A. MATHEMATICAL MODEL OF SHIP

This study uses three different coordinate systems to describe the motion equations of ships (Fig. 1).

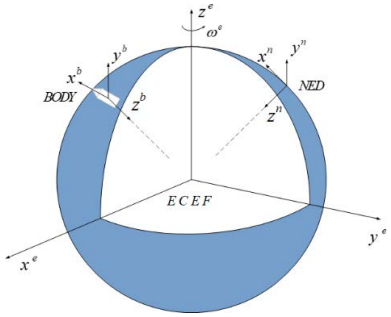

FIGURE 1. Coordinate systems used to describe the motion of a ship.

$O-x^e y^e z^e$	Earth Centered Earth Fixed coordinate system.
$O-x^n y^n z^n$	North-East-Down (NED) coordinate system.
$O-x^b y^b z^b$	Body Fixed coordinate system.

The ship's motion equation is derived from the Newtonian theory of momentum and moment of momentum, described by the body's fixed coordinate system to calculate the force and moment acting on the ship. The origin of the attached coordinate system is set at the ship's centroid, and the MMG model is established referring to the study by Yasukawa and Yoshimura [22]. Nonlinear differential equations describing the ship's heading and roll motion are as follows:

$$\begin{aligned}
(m+m_x)\,\dot{u} - \left(m+m_y\right) vr &= X_\Sigma,\\
\left(m+m_y\right)\dot{v} + (m+m_x)\,ur - mh\dot{p} &= Y_\Sigma,\\
J_z\dot{r} &= N_\Sigma,\\
\dot{\psi} &= r,\\
J_x\dot{p} - mh\dot{v} - mz_k ur &= K_\Sigma,\\
\dot{\theta} &= p,
\end{aligned} \tag{1}$$

where m is the ship's mass, m_x, m_y are the additional mass of the hull longitudinal and transverse, h is the metacentric height of the ship, z_k is the length of the inertia moment arm, u, v, p, r are the ship's surge velocity, sway velocity, roll angular velocity, and heading angular velocity, J_x, J_z are the projection of the hull's additional moment of inertia on the x-axis and z-axis of the body-fixed coordinate system, $X_\Sigma, Y_\Sigma, K_\Sigma, N_\Sigma$ are the projection of the forces and moments acting on the ship on the axes of the body-fixed coordinate system. The following formula determines these projections:

$$\begin{aligned} X_\Sigma &= 1.8T - X_H - X_R + f_x, \\ Y_\Sigma &= Y_H + Y_R + f_y, \\ K_\Sigma &= M_{XH} + M_{XR} + M_{XRB} + M_X, \\ N_\Sigma &= M_{YH} + M_{YR} + M_Z, \end{aligned} \tag{2}$$

where X_H, Y_H, M_{XH}, M_{YH} are the viscous hydrodynamic forces and moments acting on the ship's hull, X_R, Y_R, M_{XR}, M_{YR}, M_{XRB} are the forces and moments generated by the deflection of the vertical rudder and fins, T is the thrust of the propeller, f_x, f_y, M_X, M_Z are the external disturbance forces and moments.

The nonlinear mathematical model accurately describes the ship's motion and is suitable for testing the controller's performance, but it is difficult to use for controller design [23]. Therefore, there is a need to linearize the mathematical model of the ship's motion to design the controller. According to Blanke and Christensen [24], taking the ship's surge velocity as a constant value, the motion of $[v, r, \psi, p, \theta]$ near the system equilibrium operating point, the linear mathematical model of the ship's motion is summarized as the following:

$$\begin{aligned} \begin{bmatrix} \dot{v} \\ \dot{r} \\ \dot{\psi} \\ \dot{p} \\ \dot{\theta} \end{bmatrix} &= \begin{bmatrix} a_{11} & a_{12} & 0 & a_{14} & a_{15} \\ a_{21} & a_{22} & 0 & 0 & 0 \\ 0 & 1 & 0 & 0 & 0 \\ a_{41} & a_{42} & 0 & a_{44} & a_{45} \\ 0 & 0 & 0 & 1 & 0 \end{bmatrix} \begin{bmatrix} v \\ r \\ \psi \\ p \\ \theta \end{bmatrix} \\ &+ \begin{bmatrix} b_{11} & b_{12} \\ b_{21} & 0 \\ 0 & 0 \\ b_{41} & b_{42} \\ 0 & 0 \end{bmatrix} \begin{bmatrix} \delta_v \\ \delta_b \end{bmatrix} + \begin{bmatrix} h_{11} & 0 & h_{13} \\ 0 & h_{22} & 0 \\ 0 & 0 & 0 \\ h_{41} & 0 & h_{43} \\ 0 & 0 & 0 \end{bmatrix} \\ &\times \begin{bmatrix} f_y \\ M_Z \\ M_X \end{bmatrix}, \end{aligned} \tag{3}$$

$$\begin{bmatrix} \psi \\ \theta \end{bmatrix} = \begin{bmatrix} 0 & 0 & 1 & 0 & 0 \\ 0 & 0 & 0 & 0 & 1 \end{bmatrix} \begin{bmatrix} v \\ r \\ \psi \\ p \\ \theta \end{bmatrix}. \tag{4}$$

The above state space model can be simplified as:

$$\begin{aligned} \dot{x} &= Ax + B\Delta + Hf, \\ y &= Cx, \end{aligned} \tag{5}$$

where $x = [v, r, \psi, p, \theta]^T$ is the state vector, y is the output vector, $\Delta = [\delta_v, \delta_b]^T$ is the control vector, and $[\delta_v, \delta_b]$ are rudder and fin angles respectively. $f = \left[f_y, M_Z, M_X\right]^T$ is the external interference vector. A is the state matrix, determined by the sailing speed, mass, moment, and hydrodynamic coefficient B is the input matrix, determined by the sailing speed, the position of the rudder and fins, C is the output matrix. H is the external disturbance matrix determined by the external disturbance wave characteristics and the sailing speed.

B. ACTUATOR MODEL

The dynamic characteristics of the actuator are closely related to the controller's design. The dynamic characteristics of its mathematical model should be consistent with those of the actual physical device [25], [26].

- Maximum rudder/fin angle limit: $|\Delta| \le \Delta_c$.
- Maximum rudder/fin angular rate limit: $\left|\dot{\Delta}\right| \le \dot{\Delta}_c$.

where $\Delta_d = [\delta_{vd}, \delta_{bd}]$ is the command rudder/fin angle,$\Delta = [\delta_v, \delta_b]$ is the rudder/fin deflection angle, $\Delta_c = [\delta_{vc}, \delta_{bc}]$ is the upper limit of rudder/fin deflection angle (for vertical rudder $\delta_{vc} = 30^\circ$, for stabilizer fin $\delta_{bc} = 35^\circ$), $\dot{\Delta} = [\dot{\delta}_v, \dot{\delta}_b]$ is the velocity of rudder/fin deflection, $\dot{\Delta}_c = [\dot{\delta}_{vc}, \dot{\delta}_{bc}]$ is the upper limit of rudder/fin deflection angular velocity (for vertical rudder $\dot{\delta}_{vc} = 3^\circ/s$, for fin stabilizer $\dot{\delta}_{bc} = 35^\circ/s$). The mathematical model of actuator is shown in Fig. 2.

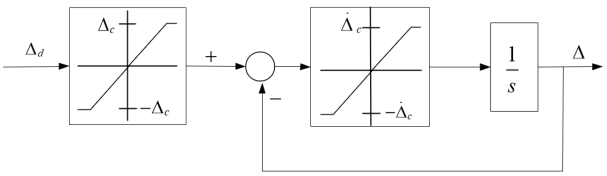

FIGURE 2. Mathematical model of actuator.

C. WAVE DISTURBANCE MODEL

This paper adopts rational spectrum modeling to simulate wave interference [27]. $S_\gamma(\omega)$ is the power spectral density function of wave inclination $\chi(t)$. The power spectral density function $S_\gamma(\omega)$ and its corresponding correlation function $K_\gamma(\tau)$ are determined by equation (6):

$$\begin{aligned} S_\gamma(\omega) &= \frac{4D_r\alpha\omega^2}{\omega^4 + 2\left(\alpha^2 - \beta^2\right)\omega^2 + \left(\alpha^2 + \beta^2\right)^2}, \\ K_\gamma(\tau) &= D_r\sqrt{1 + (\alpha/\beta)^2}e^{\alpha|\tau|}\cos\left(\beta\tau + \tan^{-1}(\alpha/\beta)\right), \end{aligned} \tag{6}$$

where D_r is the discrete difference of the longitudinal distance of the wave. α is the damping coefficient and $\beta$is the frequency angle of the correlation function. The spectrum signal in the form of equation (6) is formed by filtering single white noise through a wave-forming filter in equation (7):

$$\begin{aligned} G(s) &= \frac{2\sqrt{\alpha D_r}s}{s^2 + 2\alpha s + \left(\alpha^2 + \beta^2\right)}, \\ D_r &= 0.0358h_{3\%}^2, \quad \beta = \omega_m, \ \alpha = 0.1\beta. \end{aligned} \tag{7}$$

The highest frequencies of the approximate spectrum and $h_{3\%}^2$ (3% meaningful wave height) in equation (7) are determined in Table 1.

TABLE 1. Meaningful wave heights and approximate spectral maximum frequencies corresponding to different wave levels.

Sea level	1	2	3	4	5	6	7	8	9
$h_{3\%}^2$	0	0.25	0.75	1.25	2.00	3.50	6.00	8.50	11.0
ω_m	1.0	0.82	0.70	0.57	0.53	0.50	0.48	0.46	0.44

III. CONTROLLER DESIGN

This section introduces the composition and design of the controller. The state observer can reconstruct the system's state vector, and the LQR can obtain the optimal solution to the governing equation. This paper improves the traditional LQR and designs a dynamic corrector to reduce the ship roll angle and the heading angle deviation caused by wave disturbance to achieve a better control effect.

A. STATE OBSERVER

The system's state vector is difficult to obtain directly, but the state vector is required for actual control [28]. Therefore, a state observer (Fig. 3) can be designed to obtain the estimated value of the system's state vector via input and output. When the external disturbance is not considered, the state space formal motion equation of the ship can be expressed as follows:

$$\begin{aligned} \dot{x} &= Ax + B\Delta, \\ y &= Cx. \end{aligned} \tag{8}$$

The closed-loop state observer equation is designed as follows:

$$\dot{\hat{x}} = A\hat{x} + B\Delta + G(y - C\hat{x}), \tag{9}$$

where $\hat{x}$ is an estimate of the state vector x, G is the observation coefficient matrix.

$$x = \begin{pmatrix} v \\ r \\ \psi \\ p \\ \theta \end{pmatrix}, \quad \hat{x} = \begin{pmatrix} \hat{v} \\ \hat{r} \\ \hat{\psi} \\ \hat{p} \\ \hat{\theta} \end{pmatrix}, \quad \Delta = \begin{pmatrix} \delta_v \\ \delta_b \end{pmatrix}, \quad y = \begin{pmatrix} \psi \\ \theta \end{pmatrix},$$

$$G = \begin{pmatrix} g_1 & 0 \\ g_2 & 0 \\ g_3 & 0 \\ 0 & g_4 \\ 0 & g_5 \end{pmatrix}.$$

If we introduce the deviation vector $\varepsilon = x - \hat{x}$, then according to equations (8) and (9), we can get:

$$\dot{\hat{x}} - \dot{x} = (A - GC)\left(\hat{x} - x\right). \tag{10}$$

By configuring $g_1 \sim g_5$ in the matrix $(A - GC)$ so that all eigenvalues have negative real parts, then $t \to \infty, \varepsilon = 0$, and the estimated vector $\hat{x}$ is approximately equal to the state vector x. When assigning the characteristic values of $(A - GC)$ by assigning poles, it is important to consider the rate of $\hat{x}$ converging to x and the passband of the state observer so that it has a certain anti-interference ability.

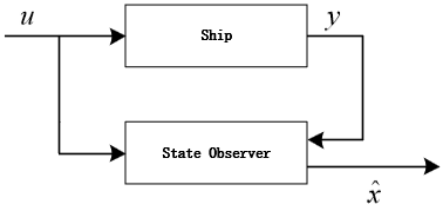

FIGURE 3. State observer.

B. RATE CONTROL LAW WITH NO STATIC ERROR

Considering the static disturbance of the closed-loop system, the control law obtained using classical LQR cannot guarantee the free static error of the closed-loop system. This paper proposes a rate control law with no static error based on the optimal control law obtained using LQR [29], [30]. First, the state quantity of the above motion state space model is extended by introducing the input quantity Δ:

$$\begin{bmatrix} \dot{v} \\ \dot{r} \\ \dot{\psi} \\ \dot{p} \\ \dot{\theta} \\ \dot{\delta}_v \\ \dot{\delta}_b \end{bmatrix} = \begin{bmatrix} a_{11} & a_{12} & 0 & a_{14} & a_{15} & b_{11} & b_{12} \\ a_{21} & a_{22} & 0 & 0 & 0 & b_{21} & 0 \\ 0 & 1 & 0 & 0 & 0 & 0 & 0 \\ a_{41} & a_{42} & 0 & a_4 & a_{45} & b_{41} & b_{42} \\ 0 & 0 & 0 & 1 & 0 & 0 & 0 \\ 0 & 0 & 0 & 0 & 0 & 0 & 0 \\ 0 & 0 & 0 & 0 & 0 & 0 & 0 \end{bmatrix} \times \begin{bmatrix} v \\ r \\ \psi \\ p \\ \theta \\ \delta_v \\ \delta_b \end{bmatrix} + \begin{bmatrix} 0 & 0 \\ 0 & 0 \\ 0 & 0 \\ 0 & 0 \\ 0 & 0 \\ 1 & 0 \\ 0 & 1 \end{bmatrix} \begin{bmatrix} \dot{\delta}_v \\ \dot{\delta}_b \end{bmatrix}. \tag{11}$$

The equation of state of the extended system is:

$$\dot{\tilde{x}} = \tilde{A}\tilde{x} + \tilde{B}\dot{\Delta}, \tag{12}$$

where $\tilde{x} = [v, r, \psi, p, \theta, \delta_v, \delta_b]^T$, $\tilde{A}, \tilde{B}$ are the matrix augmented from A, B. Second, the traditional LQR is designed, and the indicator functional is:

$$J = \frac{1}{2}\int_0^T \tilde{x}^T Q\tilde{x} + u_{LQR}^T R u_{LQR} dt, \tag{13}$$

where the weighting matrices Q and R are positive definite symmetric matrices and u_{LQR} is the input vector. The obtained u_{LQR} minimizes the functional by solving the algebraic Riccati equation.

$$P\tilde{A} + \tilde{A}^T P - P\tilde{B}R^{-1}\tilde{B}^T P + Q = 0, \tag{14}$$

where $\tilde{A}, \tilde{B}, Q, R$ are constant matrices, P is the symmetric positive definite solution of algebraic Riccati equation. When $t \to \infty$, the system can be completely controlled and observed, the optimal control is u^*_{LQR}.

$$u^*_{LQR} = -R^{-1}\tilde{B}P\tilde{x}. \tag{15}$$

The control law structure obtained based on the LQR is shown as follows:

$$u^*_{LQR} = K\tilde{x} = K_x x + K_\Delta \Delta, \tag{16}$$

where $K = -R^{-1}\tilde{B}'P$, K_x, K_Δ are the components of K. Satisfying the following equations is a necessary and sufficient condition for a linear system to have no static error: $F_{fp}(s) = 0$, where $F_{fp}(s)$ is the transfer matrix from input f to output p. When the external disturbance f is not considered, the state space equation can be written as$\dot{x} = Ax + B\Delta$. The state vector$x$can be written as $x = \left(x_a | x_p\right)^T$, x_a andx_p are components of the state vector. The following methods are adopted to ensure the nonstatic error of the closed-loop system:

$$p = L_a x_a + L_p x_p, L = \left(L_a | L_p\right), \quad p = Lx, \tag{17}$$

where p is an adjustable variable, and an auxiliary matrix L is introduced to achieve its statically free property. Since the matrix L_p is a nonsingular matrix, we can get:

$$x_p = L_p^{-1}p - L_p^{-1}L_a x_a. \tag{18}$$

At this time, the state equation of ship motion can be written as $\dot{x} = A_a x_a + A_p x_p + B\Delta$; substituting equation (18) into it, we can get:

$$\dot{x} = \left(A_a - A_p L_p^{-1} L_a\right) x_a + B\Delta + A_p L_p^{-1} p. \tag{19}$$

The control law can be transformed by introducing auxiliary vectors $\gamma = \left(x_a | \Delta\right)^T$ and $S = \left(A_a - A_p L_p^{-1} L_a | B\right)$:

$$\begin{aligned} u^*_{LQR} &= K_x x + K_\Delta \Delta, \\ &= K_{xa} x_a + K_{xp} x_p + K_\Delta \Delta, \\ &= MS^{-1}\dot{x} + Np, \\ &= \mu\dot{x} + \nu y, \end{aligned} \tag{20}$$

where $M = \left(K_{xa} - K_{xp}L_p^{-1}L_a | K_\delta\right)$, S, N are nonsingular matrices $N = K_{xp}L_p^{-1} - MS^{-1}A_p L_p^{-1}$. The resulting control law $u^*_{LQR} = \mu\dot{x} + \nu y$ is called the rate control law with no static error, μ is the member of the matrix MS^{-1}, ν is the member of the matrix N. The above control law not only maintains the optimality of the basic law but also guarantees the nonstatic error in the system state vector. When the ship's speed $u = 12.5m/s$:

$$\mu = \begin{bmatrix} 1.02 & 11.46 & 8.59 & 0.02 & -9.85e^{-8} \\ -62.41 & -6.54 & 70.57 & -27.91 & -58.23 \end{bmatrix},$$

$$\nu = \begin{bmatrix} 1.22 & 2.25e^{-7} \\ 0 & -20.33 \end{bmatrix}.$$

C. DYNAMIC CORRECTOR

When the ship is disturbed by the waves during the navigation, it will produce sway motions in all directions. The purpose of designing a dynamic corrector is to improve the stability of the heading and roll under the disturbance of waves. The transfer matrix of the dynamic corrector should be selected to minimize the heading angle ψ and roll angle θ deviation caused by wave disturbance at each moment.

The mathematical model of the dynamic corrector is:

$$\xi = F(s)\,\zeta, \tag{21}$$

where $\zeta = y - C\hat{x}$ is the corrector input vector, ξ is the corrector output vector. The transfer matrix $F(s)$ can be obtained by the following method. The mathematical model of Fig. 4 can be described as follows:

$$\begin{aligned} \dot{\hat{x}} &= A\hat{x} + B\Delta + G(y - C\hat{x}), \\ \dot{\Delta} &= u^*_{LQR}, \\ u^*_{LQR} &= \mu\dot{x} + \nu y + \xi, \\ &= K_0\hat{x} + K_1\Delta + \nu_0 y + \xi, \end{aligned} \tag{22}$$

where $K_0 = \mu(A - GC)$, $K_1 = \mu B$, $\nu_0 = \mu G + \nu$, its state space model can be obtained as:

$$\begin{aligned} \begin{pmatrix} \dot{\hat{x}} \\ \dot{\Delta} \end{pmatrix} &= \left(\begin{array}{c|c} A - GC & B \\ \hline K_0 & K_1 \end{array}\right)\begin{pmatrix} \hat{x} \\ \Delta \end{pmatrix} + \left(\begin{array}{c|c} G & 0_{5\times 2} \\ \hline \nu_0 & E_{2\times 2} \end{array}\right)\begin{pmatrix} y \\ \xi \end{pmatrix}, \\ \begin{pmatrix} \Delta \\ \zeta \end{pmatrix} &= \left(\begin{array}{c|c} 0_{2\times 5} & E_{2\times 2} \\ \hline K_0 & K_1 \end{array}\right)\begin{pmatrix} \hat{x} \\ \Delta \end{pmatrix} + \left(\begin{array}{c|c} 0_{2\times 2} & 0_{2\times 2} \\ \hline E_{2\times 2} & 0_{2\times 2} \end{array}\right)\begin{pmatrix} y \\ \xi \end{pmatrix}. \end{aligned} \tag{23}$$

The listed mathematical model can be transformed into frequency domain form by means of input and output equations:

$$\begin{pmatrix} \Delta \\ \zeta \end{pmatrix} = T(s)\begin{pmatrix} y \\ \xi \end{pmatrix} = \left(\begin{array}{c|c} T_{11}(s) & T_{12}(s) \\ \hline T_{21}(s) & T_{22}(s) \end{array}\right)\begin{pmatrix} y \\ \xi \end{pmatrix}, \tag{24}$$

where $T_{11}(s), T_{12}(s), T_{21}(s), T_{22}(s)$ are the members of the transfer matrix $T(s)$:

$$\begin{aligned} T(s) = &\left(\begin{array}{c|c} 0_{2\times 5} & E_{2\times 2} \\ \hline -C & 0_{2\times 2} \end{array}\right)\left(E_{7\times 7}s - \left(\begin{array}{c|c} A - GC & B \\ \hline K_0 & K_1 \end{array}\right)\right)^{-1} \\ &\times \left(\begin{array}{c|c} G & 0_{5\times 2} \\ \hline \nu_0 & E_{2\times 2} \end{array}\right) + \left(\begin{array}{c|c} 0_{2\times 2} & 0_{2\times 2} \\ \hline E_{2\times 2} & 0_{2\times 2} \end{array}\right). \end{aligned} \tag{25}$$

By combining equations (21) and (24), and removing the internal variables ξ and ζ, we can obtain the transfer matrix $F_{y\Delta}(s)$ from input y to output Δ.

$$\begin{aligned} F_{y\Delta}(s) = &T_{11}(s) + T_{12}(s)F(s) \\ &\times \left[E_2 - T_{22}(s)F(s)\right]^{-1} T_{21}(s). \end{aligned} \tag{26}$$

Similarly $F_{yf}(s)$ is the transfer function from the input external disturbance to the output y. We can derive the transfer function $F_{yf}(s)$ from the transfer function $F_{y\Delta}(s)$:

$$F_{yf}(s) = C\left[Es - A - BF_{y\Delta}(s)C\right]^{-1}H. \tag{27}$$

The problem of optimal suppression of the influence of input on the output is equivalent to the minimization of some

matrix norm of the transfer function. The deviation values of ψ and θ caused by the external disturbance of the ocean wave are minimized by adjusting the controllable matrix $F(s)$ in the transfer function $F_{yf}(s)$.

$$y = F_{yf}(s)f, \tag{28}$$

where $y = [\psi, \theta]^T, f = \left[f_y, M_Z, M_X\right]^T$. Define the functional:

$$\begin{aligned} J(F) &= \left\| F_{yf}(s, F(s)) \right\|_{2S} \\ &= \sqrt{\frac{1}{2\pi} \int_{+\infty}^{-\infty} tr\left[F_{yf}(j\omega) S_\gamma(\omega) F_{yf}(-j\omega)\right] d\omega}, \\ &\quad \times \left\{ F(s) \in \Omega : F_{yf}(s, F(s)) \le \delta_0 \right\}, \end{aligned} \tag{29}$$

where δ_0 is the control intensity limit, defined by a given normal number. The optimal solution is obtained by the following method:

$$J \to \min_{F(s)\in\Omega}, \quad J_{\min} = \min_{F(s)\in\Omega} J(F), \; F(s) = \arg J_{\min}.$$

The $F(s)$ obtained at this time is the optimal transfer matrix of the dynamic corrector.

D. CONTROLLER

The block diagram of the controller is shown in the dotted box in Fig. 4, composed of a state observer, dynamic corrector, and rate control law with no static error.

State observer equation:

$$\dot{\hat{x}} = A\hat{x} + B\Delta + G(y - C\hat{x}). \tag{30}$$

Dynamic corrector equation:

$$\xi = F(s)\left(\psi - \hat{x}_3 \middle| \theta - \hat{x}_5\right)^T. \tag{31}$$

Rate control law with no static error:

$$\begin{aligned} u_v &= \mu_1 \dot{\hat{x}} + v_{11}(\psi - \psi_z) + v_{12}(\theta - \theta_z) + \xi, \\ u_b &= \mu_2 \dot{\hat{x}} + v_{22}(\theta - \theta_z) + \xi, \\ \dot{\delta}_v &= u_v, \\ \dot{\delta}_b &= u_b, \end{aligned} \tag{32}$$

where u_v, u_b is the rudder/fin control law, μ_1, μ_2 are members of the matrix MS^{-1}, v_{11}, v_{12}, v_{22} are members of the matrix N, ξ is the output of the dynamic corrector.

IV. SIMULATION RESULTS

A. SIMULATION ENVIRONMENT

In this paper, a ship with a length of 134 m is selected for simulation. The main parameters of the ship are shown in Table 2. In the following simulation, the speed of the ship $u = 12.5$ m/s and wave angle $\psi_\omega = 45°$. Fig. 5 shows the MATLAB simulation environment built to simulate the control system, test the roll and heading stability of the ship, and verify the control performance of the improved control algorithm.

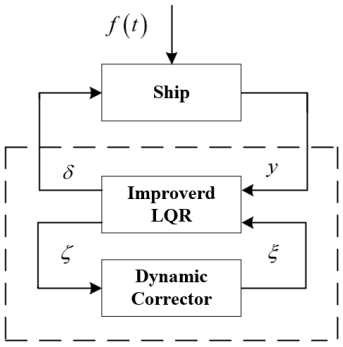

FIGURE 4. Block diagram of the controller.

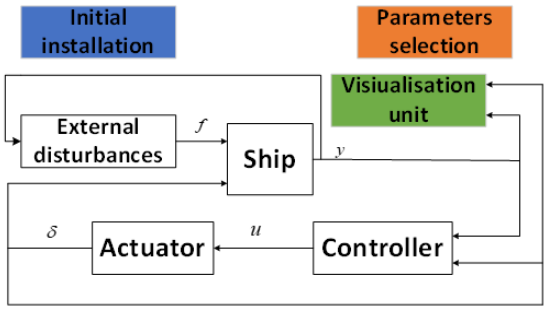

FIGURE 5. MATLAB simulation environment.

The initialization module is used to initialize the data before the simulation starts. The parameter selection module is used to configure the parameters of the controller. The external interference module is composed of a wave interference mathematical model. The actuator comprises a vertical rudder and a fin stabilizer transmission model. The controller consists of a closed-loop state observer, dynamic corrector, and rate control law with no static error. The visualization module monitors the system state variables in real time.

TABLE 2. The main parameters of the simulation ship.

parameters	value	symbol
Length	134.00 m	L
Beam	16.60 m	B
Draft	5.44 m	d
Displacement	4500 m^3	W
Transverse metacenter height	1.11 m	h
Inertia arm	4.57 m	z_k

B. VERIFY THE CONTROL LAW OF ASTAIC

By applying static interference $\left(f_y = 5, M_x = 0, M_z = 800\right)$ to ship to verify the validity of the rate control law with no static error. Fig. 6 shows the heading angle when the step response is 15 under three control methods. Table 3 shows output of the three control methods at the end of the response.

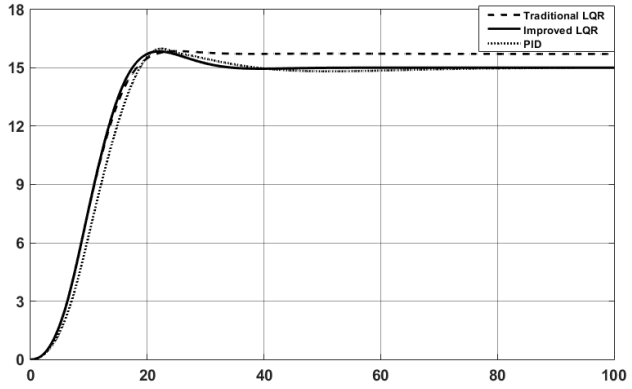

FIGURE 6. Heading angle when the step response is 15 under three control methods.

TABLE 3. Output of the three control methods at the end of the response.

Time (s)	PID	Traditional LQR	Improved LQR
40	14.96°	15.71°	14.95°
60	14.85°	15.72°	15.00°
80	14.97°	15.71°	15.00°
100	15.00°	15.71°	15.00°

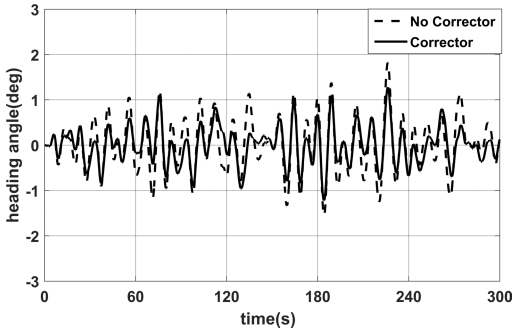

FIGURE 7. Comparison of course stability with dynamic correction (on/off) at level 3 sea state.

The simulation results show that compared with PID, the improved LQR has similar static error elimination effect, can reach the stable value faster with less overshoot. Compared with the traditional LQR static error elimination effect is better, there is little difference in overshoot. In addition, the PID algorithm has poor anti-interference ability and is suitable for SISO system. Comprehensive consideration, the improved LQR is more suitable for the design of the fin-rudder joint controller.

C. PERFORMANCE OF THE DYNAMIC CORRECTOR

A comparative experiment is performed by setting the dynamic corrector switch in the controller to analyze the effect of adding a dynamic corrector to the improved control law. Figs. 7–10 show the ship roll angle and course stability under class 3 and class 5 sea conditions, respectively. Table 4 lists the standard deviations of ship roll and heading angles with dynamic corrector (on/off) at level sea 3 and 5 states.

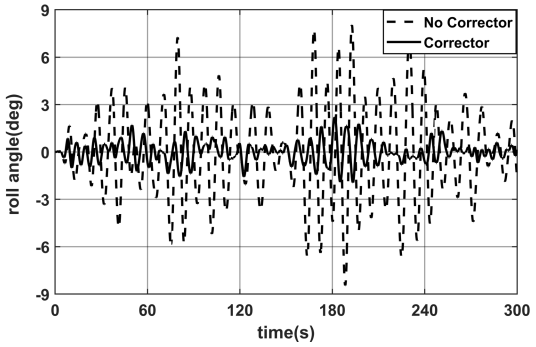

FIGURE 8. Comparison of roll stability with dynamic correction (on/off) at level 3 sea state.

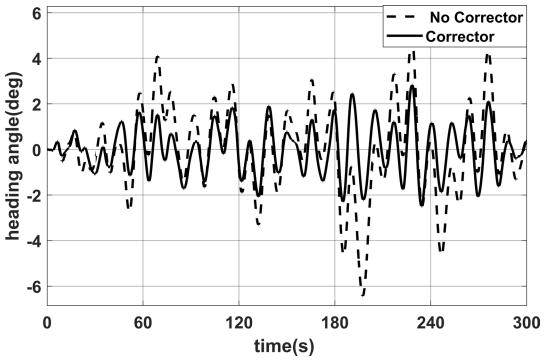

FIGURE 9. Comparison of course stability with dynamic correction (on/off) at level 5 sea state.

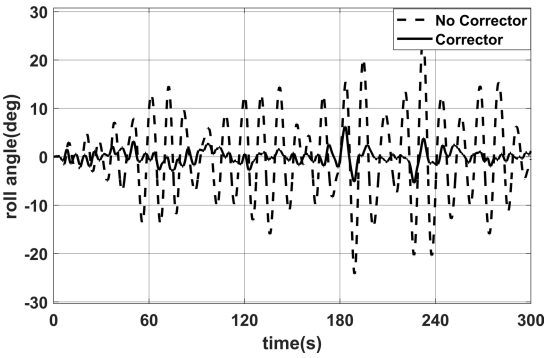

FIGURE 10. Comparison of roll stability with dynamic correction (on/off) at level 5 sea state.

TABLE 4. Standard deviations of ship roll and heading angles with dynamic corrector (on/off) at level sea 3 and 5 states.

Std	Corrector Off (3)	Corrector On (3)	Corrector Off (5)	Corrector On (5)
σ_θ	2.89	0.68	8.14	1.58
σ_ψ	0.59	0.41	1.94	1.07

In the Table 4, the standard deviation σ_θ and σ_ψ are used to measure the error of the roll angle and the heading angle

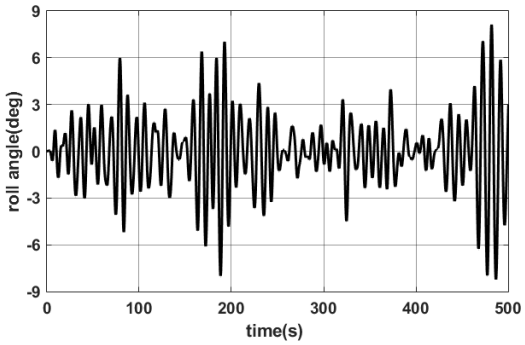

FIGURE 11. Roll stabilization performance of rudder at level 3 sea state.

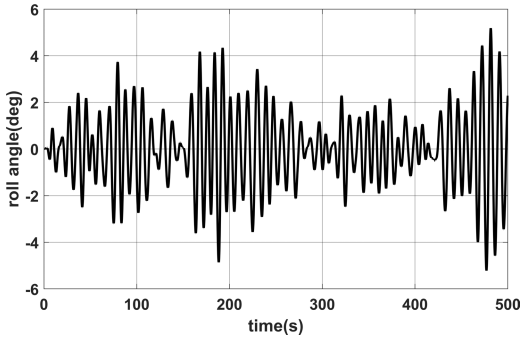

FIGURE 12. Roll stabilization performance of fin stabilizer at level 3 sea state.

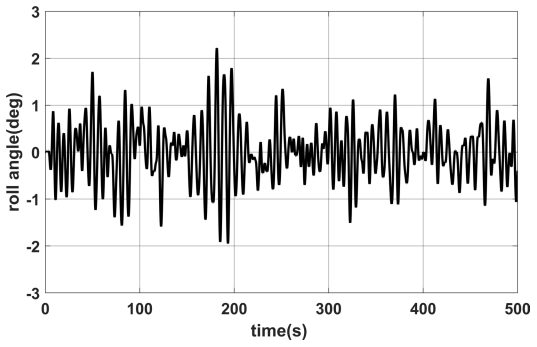

FIGURE 13. Roll stabilization performance of fin-rudder joint control at level 3 sea state.

of the ship when the ship is disturbed. The simulation results show that the designed dynamic corrector effectively reduces the influence of wave disturbance on heading angle and roll angle.

D. ROLL STABILITY PERFORMANCE

To verify the roll stability performance of the fin-rudder joint controller, comparative experiments of fin-rudder joint, fin, and rudder roll reductions were conducted at levels 3 and 5 sea states (Figs. 11–16).

When the ship is not connected to the controller at level 3 and 5 sea states, the standard deviations of roll Angle are $\sigma_{\theta 3} = 3.11, \sigma_{\theta 5} = 8.34$. According to the simulation results, the fin-rudder joint control was found to have a better antiroll

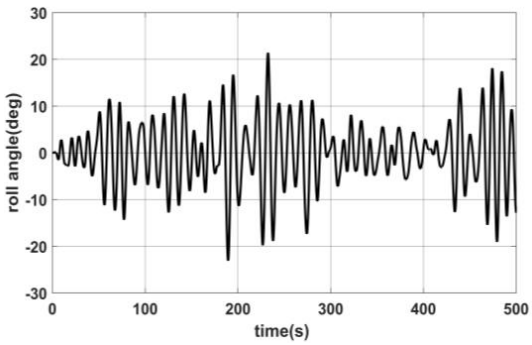

FIGURE 14. Roll stabilization performance of rudder at level 5 sea state.

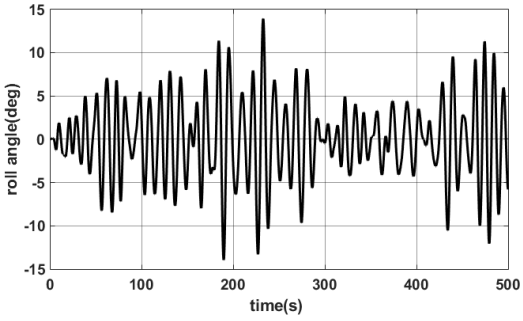

FIGURE 15. Roll stabilization performance of fin stabilizer at level 5 sea state.

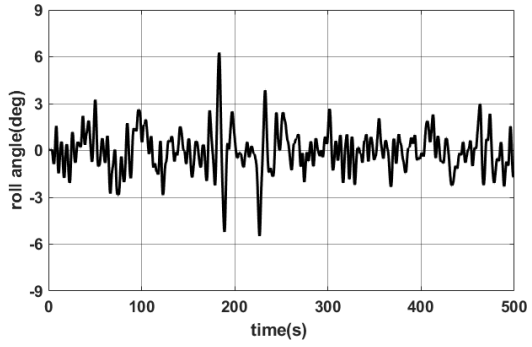

FIGURE 16. Roll stabilization performance of fin-rudder joint control at level 5 sea state.

TABLE 5. Standard deviation of ship roll Angle under three control modes at level 3 sea state.

Std	rudder	fin stabilizer	fin-rudder joint control
σ_θ	2.34	1.58	0.63

TABLE 6. Standard deviation of ship roll Angle under three control modes at level 5 sea state.

Std	rudder	fin stabilizer	fin-rudder joint control
σ_θ	7.22	4.41	1.41

effect than the single fin or rudder control, and can achieve more than 80% roll reduction effect at level 3 and 5 sea states.

E. HEADING CONTROL PERFORMANCE

The fin-rudder joint controller ensures the antiroll effect and maintains the heading. To verify the heading control performance of the fin-rudder joint controller, comparative experiments of joint fin-rudder control and rudder control were conducted at level 3 and 5 sea states respectively (Figs. 17 and 18).

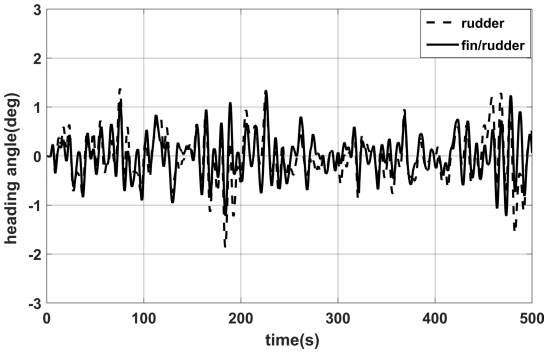

FIGURE 17. Comparison of the heading stability of the ship under rudder control and fin-rudder joint control at level 3 sea state.

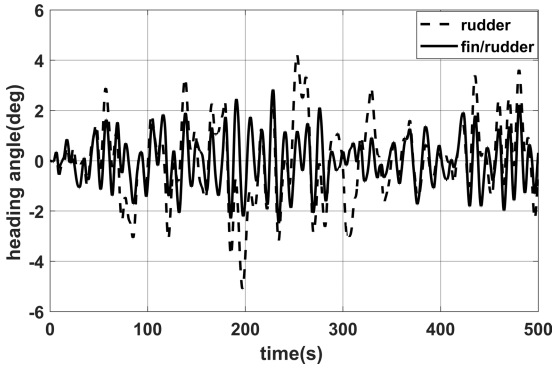

FIGURE 18. Comparison of the heading stability of the ship under rudder control and fin-rudder joint control at level 5 sea state.

TABLE 7. Standard deviation of the ship heading angles under rudder and fin-rudder joint control at level 3 and 5 sea states.

Std	rudder sea state 3	fin-rudder sea state 3	rudder sea state 5	fin-rudder sea state 5
σ_ψ	0.48	0.41	1.60	1.00

The above experimental results show that the designed fin-rudder joint controller has better course keeping ability compared with the rudder control.

V. CONCLUSION

This paper proposes a rate control with no static error based on the traditional LQR by comparing it with LQR and PID control. The dynamic corrector is designed and verified to effectively filter the influence of wave disturbance on the roll angle and heading angle. Finally, it is demonstrated that the designed fin-rudder controller effectively reduces rolling and improves ship heading stability when disturbed by waves.

REFERENCES

[1] Z. Linghui, Z. Gang, L. Wenkui, C. Yongbing, and Y. Polan, "Analysis and research on performance index function of combined rudder-fin anti-rolling based on optimal control," *Ship Sci. Technol.*, vol. 40, no. 4, pp. 17–21, 2018.

[2] T. Awad, M. A.-E. Elgohary, and T. E. Mohamed, "Ship roll damping via direct inverse neural network control system," *Alexandria Eng. J.*, vol. 57, no. 4, pp. 2951–2960, Dec. 2018.

[3] Q. Zhang, N. Jiang, Y. Hu, and D. Pan, "Design of course-keeping controller for a ship based on backstepping and neural networks," *Int. J. e-Navigat. Maritime Economy*, vol. 7, pp. 34–41, Jun. 2017.

[4] Z. Zhang, Y. Zhao, G. Zhao, H. Wang, and Y. Zhao, "Path-following control method for surface ships based on a new guidance algorithm," *J. Mar. Sci. Eng.*, vol. 9, no. 2, p. 166, Feb. 2021.

[5] I. A. Jimoh, I. B. Küçükdemiral, and G. Bevan, "Fin control for ship roll motion stabilisation based on observer enhanced MPC with disturbance rate compensation," *Ocean Eng.*, vol. 224, Mar. 2021, Art. no. 108706.

[6] S. Karakas, E. Ucer, and E. Pesman, "Control design of fin roll stabilization in beam seas based on Lyapunov's direct method," *Polish Maritime Res.*, vol. 19, no. 2, pp. 25–30, Jan. 2012.

[7] S. Jiguang, L. Lihua, Z. Songtao, and W. Jiming, "Design and experimental investigation of a GA-based control strategy for a low-speed fin stabilizer," *Ocean Eng.*, vol. 218, Dec. 2020, Art. no. 108234.

[8] M.-C. Fang, Y.-H. Lin, and B.-J. Wang, "Applying the PD controller on the roll reduction and track keeping for the ship advancing in waves," *Ocean Eng.*, vol. 54, pp. 13–25, Nov. 2012.

[9] Z. Ning, "Ship roll reduction device and its application," *Ship Eng.*, vol. 54, no. A2, pp. 271–277, 2012.

[10] R. Taggart, "Anomalous behavior of merchant ship steering systems," *Mar. Technol. SNAME News*, vol. 7, no. 2, pp. 205–215, Apr. 1970.

[11] L. Liang and Y. Wen, "Rudder roll stabilization with disturbance compensation model predictive control," *J. Mar. Sci. Technol.*, vol. 24, no. 1, pp. 249–259, Mar. 2019.

[12] J. B. Carley and A. Duberley, "Design considerations for optimum ship motion control," in *Proc. 3rd Ship Control Systems Symp.*, vol. 100, 1972.

[13] Z. Zhang and X. Zhang, "Course-keeping with roll damping control for ships using rudder and fin," *J. Mar. Sci. Technol.*, vol. 26, no. 3, pp. 872–882, Sep. 2021.

[14] J. Hongzhang, "Optimal design of rudder/fin joint control system with integral signal," *Shipbuilding China*, no. 3, p. 10, 1989.

[15] L. Ma, J. X. Xu, and G. F. Wang, "Fin/rudder joint roll reduction control system design," *Appl. Mech. Mater.*, vols. 220–223, pp. 1091–1094, Nov. 2012.

[16] H. Li, X. Pan, and C. Guo, "SMC for rudder/fin joint roll stabilization based on input-output feedback linearization," in *Proc. 36th Chin. Control Conf. (CCC)*, Jul. 2017, pp. 850–855, doi: 10.23919/ChiCC.2017.8027451.

[17] L. Liang and Y. Wen, "Disturbance compensation model predictive control for integrated rudder/fin roll stabilization," in *Proc. 37th Chin. Control Conf. (CCC)*, 2018, pp. 3859–3864, doi: 10.23919/ChiCC.2018.8482809.

[18] M. Islam and M. Okasha, "A comparative study of PD, LQR and MPC on quadrotor using quaternion approach," in *Proc. 7th Int. Conf. Mechatronics Eng. (ICOM)*, Oct. 2019, pp. 1–6, doi: 10.1109/ICOM47790.2019.8952046.

[19] J. Katebi, M. Shoaei-Parchin, M. Shariati, N. T. Trung, and M. Khorami, "Developed comparative analysis of metaheuristic optimization algorithms for optimal active control of structures," *Eng. Comput.*, vol. 36, no. 4, pp. 1539–1558, 2020.

[20] H. Zhang, F. L. Lewis, and A. Das, "Optimal design for synchronization of cooperative systems: State feedback, observer and output feedback," *IEEE Trans. Autom. Control*, vol. 56, no. 8, pp. 1948–1952, Aug. 2011, doi: 10.1109/TAC.2011.2139510.

[21] H. Zhang, F. L. Lewis, and Z. Qu, "Lyapunov, adaptive, and optimal design techniques for cooperative systems on directed communication graphs," *IEEE Trans. Ind. Electron.*, vol. 59, no. 7, pp. 3026–3041, Jul. 2012, doi: 10.1109/TIE.2011.2160140.

[22] H. Yasukawa and Y. Yoshimura, "Introduction of MMG standard method for ship maneuvering predictions," *J. Mar. Sci. Technol.*, vol. 20, no. 1, pp. 37–52, 2015.
[23] L. Liang and Y. Wen, "Integrated rudder/fin control with disturbance compensation distributed model predictive control," *IEEE Access*, vol. 6, pp. 72925–72938, 2018, doi: 10.1109/ACCESS.2018.2881752.
[24] M. Blanke and A. C. Christensen, "Rudder-roll damping autopilot robustness to sway-heading-roll couplings," Dept. Control Eng., Inst. Automat. Control Syst., DTH, Amer. Univ. Cairo, London, U.K., Tech. Rep. P93-4026, May 1994.
[25] L. Lihua, Z. Peng, Z. Songtao, J. Ming, and Y. Jia, "Simulation analysis of fin stabilizer on ship roll control during turning motion," *Ocean Eng.*, vol. 164, pp. 733–748, Sep. 2018.
[26] P. Zhao, L. Liang, S. Zhang, M. Ji, and J. Yuan, "Simulation analysis of rudder roll stabilization during ship turning motion," *Ocean Eng.*, vol. 189, Oct. 2019, Art. no. 106322.
[27] T. I. Fossen, *Handbook of Marine Craft Hydrodynamics and Motion Control: Vademecum de Navium Motu Contra Aquas et de Motu Gubernando*. Hoboken, NJ, USA: Wiley,2011.
[28] W. Chen, J. Yang, L. Guo, and S. Li, "Disturbance-observer-based control and related methods-an overview," *IEEE Trans. Ind. Electron.*, vol. 63, no. 2, pp. 1083–1095, Feb. 2016, doi: 10.1109/TIE.2015.2478397.
[29] S. Lee, K.-P. Rhee, and J.-W. Choi, "Design of the roll stabilization controller, using fin stabilizers and pod propellers," *Appl. Ocean Res.*, vol. 33, no. 4, pp. 229–239, Oct. 2011.
[30] C. Gokcek, P. T. Kabamba, and S. M. Meerkov, "An LQR/LQG theory for systems with saturating actuators," *IEEE Trans. Autom. Control*, vol. 46, no. 10, pp. 1529–1542, Oct. 2001, doi: 10.1109/9.956049.

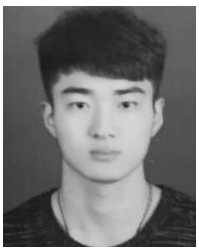

YUHAN ZHAO was born in Suihua, China, in 1997. He received the bachelor's degree in electronic information science and technology from Jilin University, Jilin, in 2019, where he is currently pursuing the M.D. degree in circuits and systems. His research interest includes ship motion control.

ZHANSHUO ZHANG was born in Changchun, China, in 1997. He received the bachelor's degree in electronic information science and technology from Jilin University, Jilin, in 2019, where he is currently pursuing the Ph.D. degree in circuits and systems. His research interests include ship motion control and ship and weather routing.

JIAWEI WANG was born in Luoyang, China, in 1999. He received the bachelor's degree in electronic information science and technology from Jilin University, Jilin, in 2022, where he is currently pursuing the Ph.D. degree in circuits and systems. His research interest includes ship motion control.

HONGBO WANG was born in Changchun, China, in 1969. She received the Ph.D. degree from Saint Petersburg State University, Russia. She is currently working with the College of Electronic Science and Engineering, Jilin University. Her research interests include ship motion control, weather routing, and ship collision avoidance.